# Reducing the Complexity of Fc Glycan Enables the Construction of Antibody Conjugates with Unexpected High Efficiency and Payload Capacity via Glycoengineering

Yang Yang[1&3], Zhentao Song[2&3], Tian Tian[1&3], Zihan Zhao[1], Ji Chen[2], Jiangping Hu[2], Xin Jiang[2], Guoli Yang[2], Qi Xue[1], Xinlu Zhao[1], Wanxing Sha[1], Yi Yang[2★], &Jie P. Li[1★]

*[1]State Key Laboratory of Coordination Chemistry, Chemistry and Biomedicine Innovation Center (ChemBIC), School of Chemistry and Chemical Engineering, Nanjing University, Nanjing 210023, China. [2]Glyco-therapy Biotechnology Co., Ltd., Building 12, Hangzhou Pharmaceutical Town, 291 Fucheng Road, Xiasha Street, Qiantang District, Hangzhou, China. [3] Contributed equally.*
★e-mail: jieli@nju.edu.cn; yiyang@glyco-therapy.com

**Glycoengineering has been demonstrated as a powerful approach to construct site-specific antibody conjugates. However, most glycoengineering strategies take of hours to days to achieve full conversion. Here, using unnatural fucosylation as an example, we show that reduce the complexity of Fc glycan dramatically boost its enzymatic conjugation. The fucosyl-biotinylation reaction on the created simple monoantennary LacNAc could be finished in 5 min while it takes 16 h on the natural biantennary LacNAc. More importantly, this unnatural fucosylation of the created simple LacNAc on antibody accommodate payloads over 15,000 Da, which allows the enzymatic construction of antibody-oligonucleotide conjugate (AOC) and bispecific antibody. Further applications of antibody conjugates in animal model and human cancer organoid indicates the translational potential of this platform, especially for constructing unlimited antibody-biomacromolecules (X) conjugate, "AXC", as therapeutics.**

Antibody conjugates are the major forms of antibody-derived macromolecules for the targeted manipulation of biological systems, which combines the exquisite specificity of antibodies with the distinct functions of payloads via chemical conjugations. Recent years have seen the great success of antibody-drug conjugate (ADC) in cancer treatment[1], especially the trastuzumab deruxtecan (T-DXd; DS-8201), an ADC composed of an anti-HER2 antibody and topoisomerase I inhibitor, which might redefine the standard therapy of HER2-low breast cancer[2]. Meanwhile, the first antibody–oligonucleotide conjugate (AOC) has entered into a phase I clinical trial last year, and this breakthrough broaden the molecular types of antibody conjugate-based drugs[3]. Beyond the therapeutic application[4], AOCs have been used in the sensitive and multiplexed detections of proteins in single cells[5] or traceless samples[6], such as the rapid measurement of protein biomarkers in minimal sample volume from patients.

It is predictable that antibody conjugates are going to be extensively expanded in the near future for a broad range of applications, including small-molecule drugs, fluorophores, catalysts, synthetic polymers[7], oligonucleotides, peptides, enzymes and other proteins, either as technical tools or clinical therapeutics[8]. Thus, the future requirements of antibody conjugation lie in satisfying the unmet need of a versatile and efficient platform that allows the construction of homogenous antibody conjugates[9, 10] with unlimited payloads.

N-linked glycan on asparagine 297 (N297) of Fc domain was found as a single and universally conserved glycosylation site of IgG molecules. This glycosylation is predominantly composed of varied amounts of N-acetylglucosamine, fucose, galactose, mannose and N-acetylneuraminic acid (sialic acid) residues, which are assembled in different complex-type biantennary structures[11]. The inherent site-specificity of Fc glycosylation make the glycoengineering being recognized as a universal and efficient approach to synthesize homogeneous antibody conjugates. Notably, due to the great translational potential, several antibody conjugates generated via glycoengineering have been translated into clinical trials by biotechnology companies. In general, current platforms mainly utilized galactosyltransferases (GalT)[12, 13], sialyltransferases (ST)[14] and endoglycosynthases (EndoGS)[15-18] derived from endoglycosidases to chemoenzymatically synthesize antibody conjugates via the Fc glycan remodeling. The payload installation via these platforms usually follows a two-step procedure, in which bioorthogonal reaction handles, *e.g.*, azide, were first introduced onto Fc via unnatural glycosylation, and drugs were further installed by bioorthogonal reactions, except the recently reported one-step EndoGS-based methods[19-21]. However, most of these platforms take hours to days to transfer small-molecule payloads (<2000 Da), and are limited to direct transfer of unnatural donor substrates bearing biomacromolecules (>10,000 Da) in one-step.

Fucose usually appears as the capping sugar in natural polysaccharides. The fucosylation reaction, in which a fucose could be transferred to the N-Acetyllactosamine (LacNAc, acceptor) from guanosine diphosphate β-L-fucose (GDP-Fuc, donor) via fucosyltransferase (FT), has not been extensively characterized to transfer fucose derivatives to the Fc glycan for the purpose of antibody conjugation. We have previously reported several cases of unnatural fucosylation to engineer cell-surface LacNAc with large payloads in minutes[22]. However, the direct use of this reaction system for synthesizing antibody glyco-conjugates is in relative low efficiency, and achieves low conversion yield in

transferring small molecular weight probes such as biotin probes (Figure S2A). Herein, we demonstrated that reducing the complexity of Fc glycan by enzymatic reactions dramatically accelerate the unnatural Fc fucosylation to install diversified functionalities (**Figure 1A**). Compared to the complex natural biantennary N-glycan, simple monoantennary disaccharide, LacNAc, on N297 of Fc could be modified via the 1,3-FT mediated fucosyl-biotinylation in much higher reaction rate (5 minutes versus 16 hours). More importantly, biomacromolecules, such as proteins (~15 KDa) and oligonucleotides (~100 nt), could be transferred to this created simple LacNAc unit on IgG in one-step. Thus, novel antibody conjugates of ADC, AOC and bispecific antibodies were then efficiently prepared using this platform with homogeneous structures. Particularly, the platform was applied for chemical synthesis of HER2/CD3 bispecific antibody[23], which allowed the recruitment of cytolytic T cells for tumor killing of human tumor organoids[24] (**Figure 1B**). Further successful applications of these conjugates demonstrated the general applicability of this platform, and offers distinct molecular entities for future therapeutics.

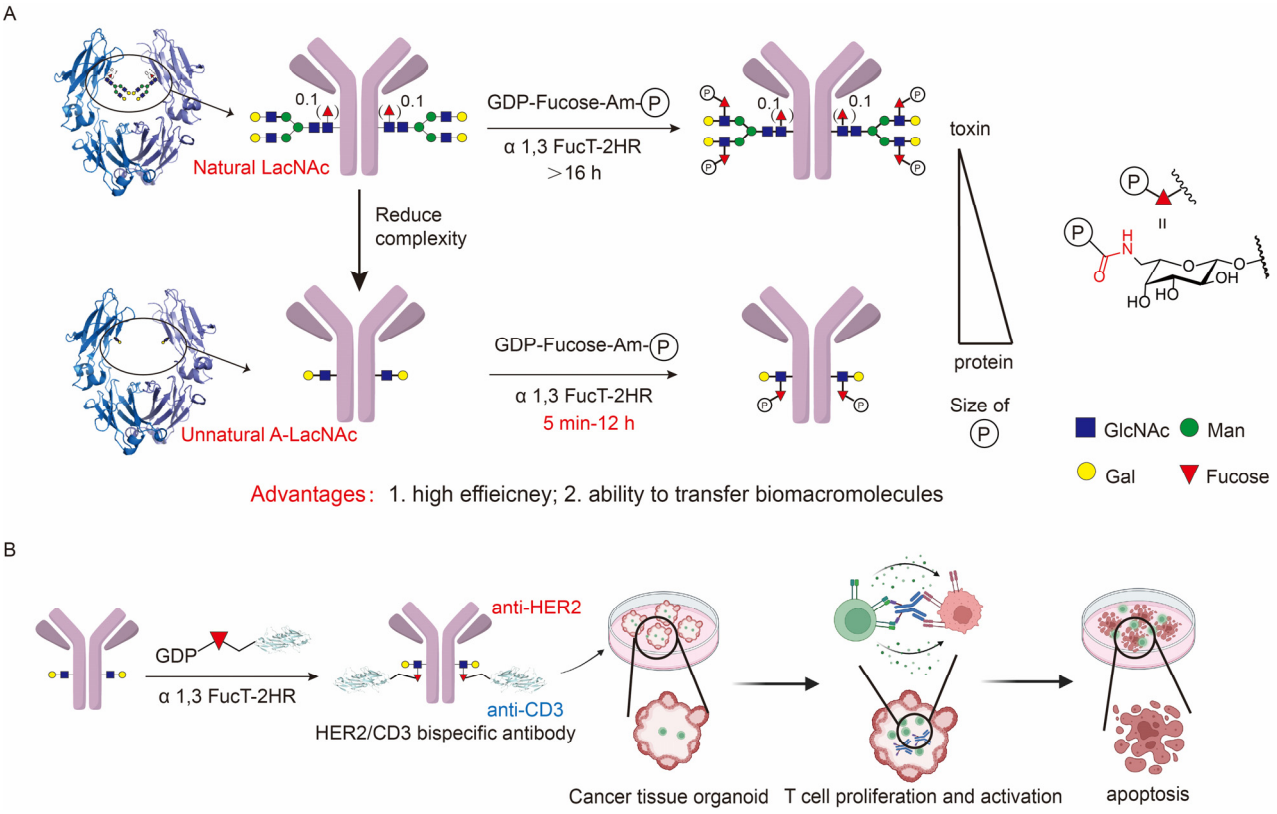


**Figure 1. Schematic illustration of LacNAc-conju platform for antibody-biomacromolecule conjugate construction.** (A) Schematic representation of enzymatic unnatural A-LacNAc labeling (LacNAc-conju) for constructing antibody conjugates. Reducing the Fc glycan complexity allows

transferring biomacromolecules to antibodies with high efficiency. (B) Chemical synthesis of HER2/CD3 bispecific antibody via LacNAc-conju enables the recruitment of cytolytic T cells for tumor killing of human tumor organoids.

## Results and discussion

### Optimization of FT mediated LacNAc labeling on natural Fc glycan of antibody

Recently, a FT enzyme originated from *H. pylori 26695*, has been reported to label LacNAc unit efficiently on cell-surface glycoproteins or glycolipids with functional moieties[22]. To transfer this reaction to modify the Fc glycan of antibody, we chose an anti-human epidermal growth factor receptor 2 (HER2) antibody, trastuzumab (Tras, also named as Herceptin), with engineered homogeneous glycan structure (G2F, four LacNAc units per antibody, see enzymatic engineering protocol in Methods) as the model protein (**Figure S1**). Using the previously reported FT enzyme and GDP-Fuc-azide derived biotin probe (triazole linker, TA), LacNAc units on G2F-Tras antibody were only partially fucosylated (~1.4 biotin per antibody) under saturated reaction conditions (5 mM GDP-Fuc-TA-biotin and 16 hours) (**Figure S2**). To achieve high efficiency of FT mediated LacNAc labeling, the linker between GDP-Fuc and payload as well as the sequence of FT enzyme were carefully optimized[25, 26]. Notably, GDP-Fuc-biotin bearing an amide linker (GDP-Fuc-AM-biotin) and a FT variant with shorter heptad repeats (FT-2HR) showed significantly improved reaction yield. As a result, we could modify G2F-Tras antibodies with almost exclusive four biotin probes via fucosylation using the improved substrate and enzyme (**Figure S3**).

### Reducing Fc glycan complexity boosts the enzymatic A-LacNAc labeling (LacNAc-conju)

Although we have achieved one-step LacNAc enzymatic labeling of biotin molecules on Fc glycan, the completion of reaction was still much longer (16 hours) (**Figure 2A**) than transferring of GDP-Fuc derivatives to the LacNAc on cell surface, which took only 10 minutes[22]. According to the crystal structure of antibody Fc domain, the glycans lied between two CH2/CH3 domains and filled the large pocket between the two CH2 domains[27] (**Figure 2B**). We envisioned that this pocket filled by the double biantennary glycans were so crowded that hinder the LacNAc enzymatic labeling. Therefore, we reduced the complexity of the Fc glycan using EndoS (an endoglycosidase for selective hydrolysis of the glycans at N297 of antibodies) and AlfC (an α-fucosidase to trim α(1,6)-fucose) to create the

GlcNAc monosaccharide on N297 via trimming the biantennary glycan and the core fucose. After that, we used Bovine β-1,4-Galactosyltransferase 1 (Y289L) ($\beta_4$GalT1) for galactosylation of the exposed GlcNAc, and created a monoantennary disaccharide structure, LacNAc, on N297 of Fc domain (hereafter named A-LacNAc due to its direct linking to the amino acid) (**Figure 2B and Figure S4**). Although three enzymes are required for the conversion, the trimming and transferring processes could be realized in one-pot by the addition of EndoS, AlfC, $\beta_4$GalT1 and Uridine diphosphate galactose (UDP-Galactose) together. After the one-pot reaction, the resulting antibodies with A-LacNAc were purified by Protein A resin and further modified with biotin moieties by GDP-Fuc-AM-biotin (**2,** 80 μM). To our surprise, the transfer of fucose-biotin to A-LacNAc reached almost 100% conversion within only 5 minutes (**Figure 2B**), which outperformed those with complex biantennary structures (need 16 hours even with 5 mM GDP-Fuc-AM-biotin) (**Figure 2A**). Finally, we monitored the conversion efficiency of natural LacNAc and A-LacNAc at different intervals with the same concentration of the substrate (Figure 2C). More than 70% A-LacNAc was converted within only 0.5 min and was almost completely converted within 5 min while only ~20% natural LacNAc was converted even after 5 h (Figure 2D). The significant enhancement of reaction efficiency indicates that the crowded structure of natural Fc glycan is the main barrier for glycoengineering, and reducing Fc glycan complexity could hugely boost the enzymatic reaction. Hereafter, we named this platform that enable the modification of the created unnatural A-LacNAc on antibody as "LacNAc-conju".

To further compare the reaction rate of LacNAc-conju with the widely used click chemistry, *e.g.*, strain promoted azide alkyne cycloaddition (SPAAC)[28], we synthesized the Tras antibody modified by a simple unnatural disaccharide bearing the azide group, as the model substrate, to react with dibenzocyclooctyne (DBCO)-biotin probe (**Figure S5**). Under the treatment with the same concentration of biotin probes, the modification of Tras antibodies with the corresponding reaction handle were characterized at different time points. To our delight, LacNAc-conju applied to A-LacNAc was completed in 45 minutes on Tras-A-LacNAc antibody while SPAAC applied to the Tras-azide antibody with similar glycan structure needed 1 hour to complete the reaction. By comparison, the fucosyl-biotinylation of natural LacNAc on biantennary glycans of Tras was almost saturated in ~28% conversion efficiency using the same reaction conditions after 16 hours. The fast kinetic of LacNAc-

conju on antibody demonstrated the power of unnatural enzymatic reaction for highly efficient modification of protein.

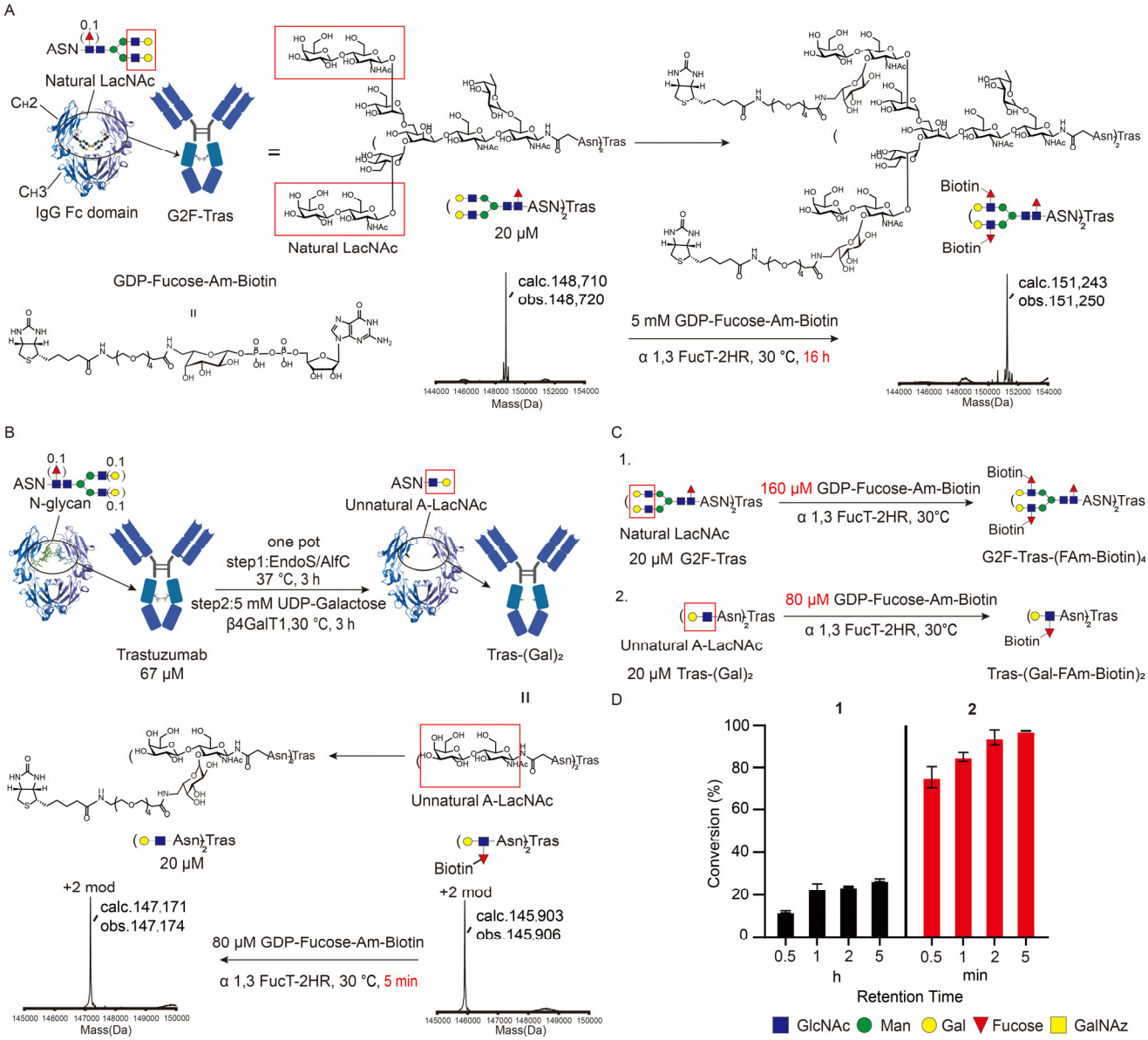


**Figure 2. Reducing the Fc glycan complexity hugely improves the efficiency of antibody glycoengineering.** (A) α 1,3 FucT-2HR mediated antibody biotinylation on the natural biantennary glycan structure (four LacNAc units per antibody) took 16 hours to complete the conversion. (B) Biantennary glycan on antibody was reengineered to generate simple monoantennary disaccharide on N297 by cascade enzymatic reactions. The reduced complexity of Fc glycan makes A-LacNAc as a more favorable substrate of α 1,3 FucT-2HR. The full antibody biotinylation on A-LacNAc only took 5 minutes with much less donor substrates. This reaction cascade could be combined in one-pot. (C-D)

The time-dependent conversion efficiency of $G_2F$-Tras-(FAm-Biotin)$_4$ (reactions 1) and Tras-(Gal-FAm-Biotin)$_2$ (reactions 2). (C) Scheme of one-step synthesis of different biotinylated Trastuzumab. Reactions (1 and 2) were performed in the presence of 20 μM substrate (G2F-Tras, Tras-(Gal)$_2$), 0.8 mg/mL enzyme in Tris buffer (25 mM, pH 7.5) at 30 °C. (D) The time-dependent conversion efficiency of different biotinylated trastuzumab. Reactions were monitored by LC-MS. (obs: Observed; calc: Calculated)

**Characterization of the trisaccharide linker of LacNAc-conju**

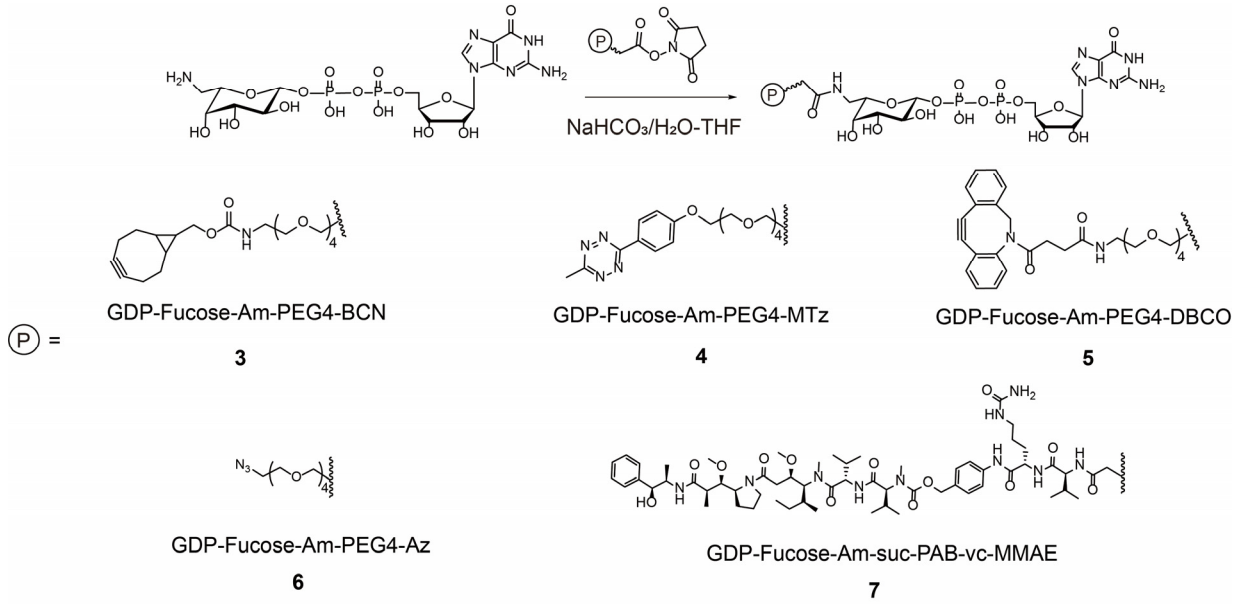


**Figure 3. Synthesis of GDP-Fuc derivatives with the amide linker.** Functional groups (payloads) include bioorthogonal handles (bicyclononyne, BCN, **3**; methyltetrazine, MTz, **4**; dibenzocyclooctyne, DBCO, **5**; azide, Az, **6**) and toxin (monomethyl auristatin E, MMAE, **7**).

To expand the functional moieties that could be introduced by LacNAc-conju, GDP-Fuc derivatives with different biorthogonal handles, such as Az, BCN, mTz and DBCO, were synthesized (**Figure 3**) and characterized by mass spectrometry, and all of them were successfully introduced to antibody with the reaction efficiency over 90% in 1 hour (**Figure S6**). Moreover, the universality of LacNAc-conju was demonstrated on several other commercially available antibodies. All the antibodies with A-LacNAc were completely unnaturally fucosylated with diversified functionalities,

indicating that the established approach was generally applicable for antibody modification **(Figure S7)**.

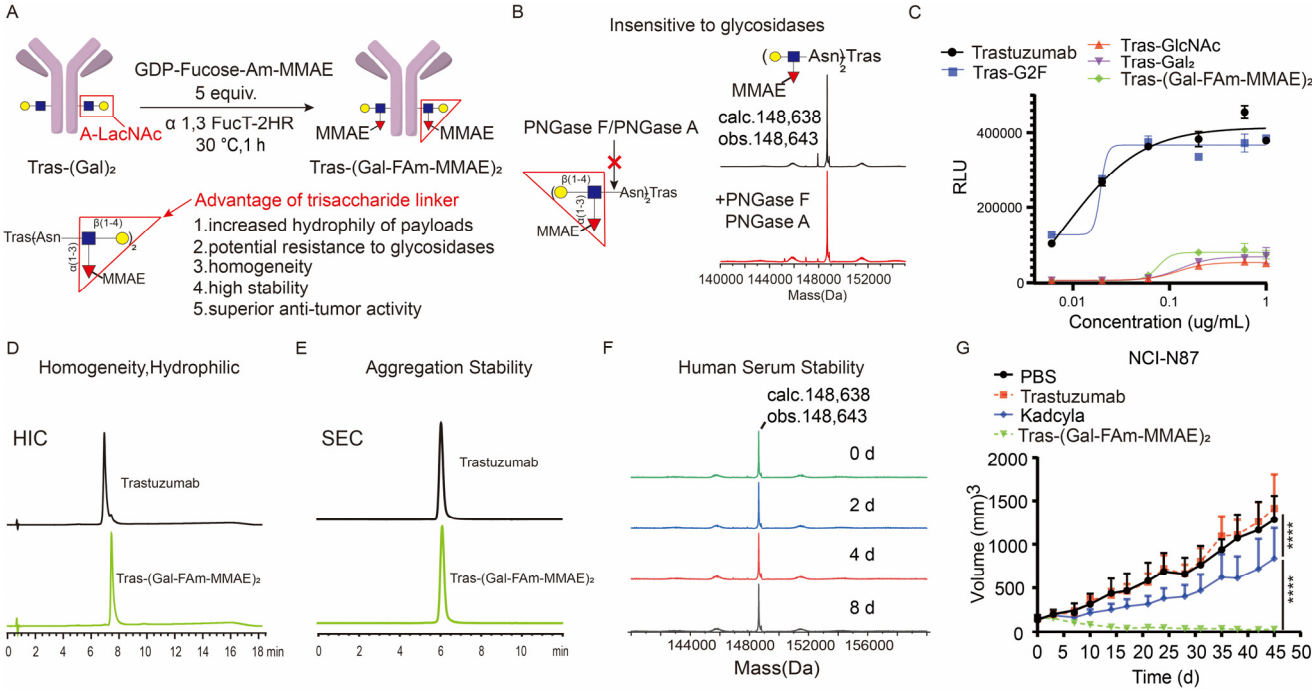


**Figure 4. Characterization of the trisaccharide linker of LacNAc-conju.** (A) Scheme of one-step synthesis of site-specific ADC, Tras-(Gal-Fam-MMAE)$_2$, using LacNAc-conju. (B) ESI-MS analysis of Tras-(Gal-FAm-MMAE)$_2$ before and after PNGase F and PNGase A treatment. (C) Antibody-dependent cellular cytotoxicity (ADCC) of different Trastuzumab glycoforms. (D-E) HIC and SEC analysis of site-specific ADCs. (D) HIC analysis of Tras-(Gal-FAm-MMAE)$_2$. (E) SEC analysis of Tras-(Gal-FAm-MMAE)$_2$. (F) ESI-MS analysis (after deconvolution) of the stability in serum after 0, 2, 4, 6, 8 days. (G) In vivo anti-tumor activity of Tras-(Gal-FAm-MMAE)$_2$ on a nude mouse human gastric NCI-N87 xenograft model Female BALB/c nude mice. Mice in different groups were *i.v.* injected with PBS, Trastuzumab (5 mg/kg), Kadcyla (5 mg/kg) and Tras-(Gal-FAm-MMAE)$_2$ (5 mg/kg) respectively when the average tumor size reached 150-200 mm$^3$ (n = 6 mice per group). The total length of the animal study was 45 days, and the tumor size and body weight of the mice were monitored twice per week throughout the experiment. (obs: Observed; calc: Calculated)

To broaden the application of LacNAc-conju, we used LacNAc-conju to create trisaccharide linkers (**Figure 4A**). For characterization, we constructed ADCs based on the created trisaccharide linker as a model. ADCs serve as a class of powerful therapeutic strategy via covalently connecting antibodies and

cytotoxic compounds for target-selective delivery of toxins into cancer cells. The toxin of monomethyl auristatin E (MMAE), conjugated to the most common cleavable linker, Val-cit-PAB (Vc-PAB), was first synthesized and modified with GDP-Fuc as described in methods (**Figure 3**). According to the previous report,[29] introducing monosaccharides or disaccharides to hydrophobic toxins could enhance the hydrophilicity and anti-tumor efficacy. Consistently, the generated GDP-Fuc derivative (GDP-Fuc-AM-VcPAB-MMAE, **7**) showed excellent hydrophilicity, and could be used to synthesize ADCs Tras-(Gal-FAm-MMAE)$_2$ via the LacNAc-conju reaction in 1 h (**Figure 4A**). Since the product of A-LacNAc fucosylation on N297 is a novel glycosylation, we characterized this trisaccharide structure via enzymatic trimming (**Figure 4B**), which coincided with the fact that neither PNGase F nor PNGase A cleaved this trisaccharide on Fc. We hypothesized that this could be attributed to the unfavorable novel glycan structure, suggesting its potential resistance to other glycosidases. Similar results were obtained for both monosaccharides and disaccharides on different types of antibodies (**Figure S8**). The created trisaccharide structure displayed enhanced antibody-dependent cellular cytotoxicity (ADCC) compared with those with monosaccharides and disaccharides (**Figure 4C**).

To further test clinically relevant property of the trisaccharide linker of LacNAc-conju, such as serum stability, the purified ADC with a trisaccharide linker was characterized by mass spectrometry (**Figure S9A**), hydrophobic interaction chromatography (HIC) and size exclusion chromatography (SEC) (**Figure 4D-E**). As a result, each antibody was labelled with two MMAE toxins uniformly, and there was no aggregation observed in the products. Moreover, the resulting ADC Tras-(Gal-FAm-MMAE)$_2$ showed high stability in human serum within 8 days (**Figure 4F**), maintained high binding capacity to HER2 antigen (**Figure S9B**), and displayed desirable high potency against HER2+ NCI-N87 cells selectively (**Figure S9C**). More importantly, Tras-(Gal-FAm-MMAE)$_2$ (DAR 2, 5 mg/kg) showed superior anti-tumor activity and induced tumor regression during 45 days in a HER2+ NCI-N87 xenograft mouse model, while the other commercial HER2-targeted ADCs Kadcyla (trastuzumab emtansine, T-DM1, DAR~4, 5 mg/kg) hardly delay tumor outgrowth (**Figure 4G**). Taken together, using ADCs as the drug model, we demonstrated both the *in vitro* and *in vivo* pharmaceutical properties of the trisaccharide linker of LacNAc-conju. Such trisaccharide linker was resistant to glycosidases and thus was highly stable in serum. Moreover, the trisaccharide linker of LacNAc-conju displayed higher

anti-tumor efficacy than commercial linkers, holding potential for the application of antibody drug synthesis synthesis.

**Use of different lengths of GDP-Fuc-ssDNA and GDP-Fucose-Am-sfGFP to test the payload capacity of LacNAc-Conju platform**

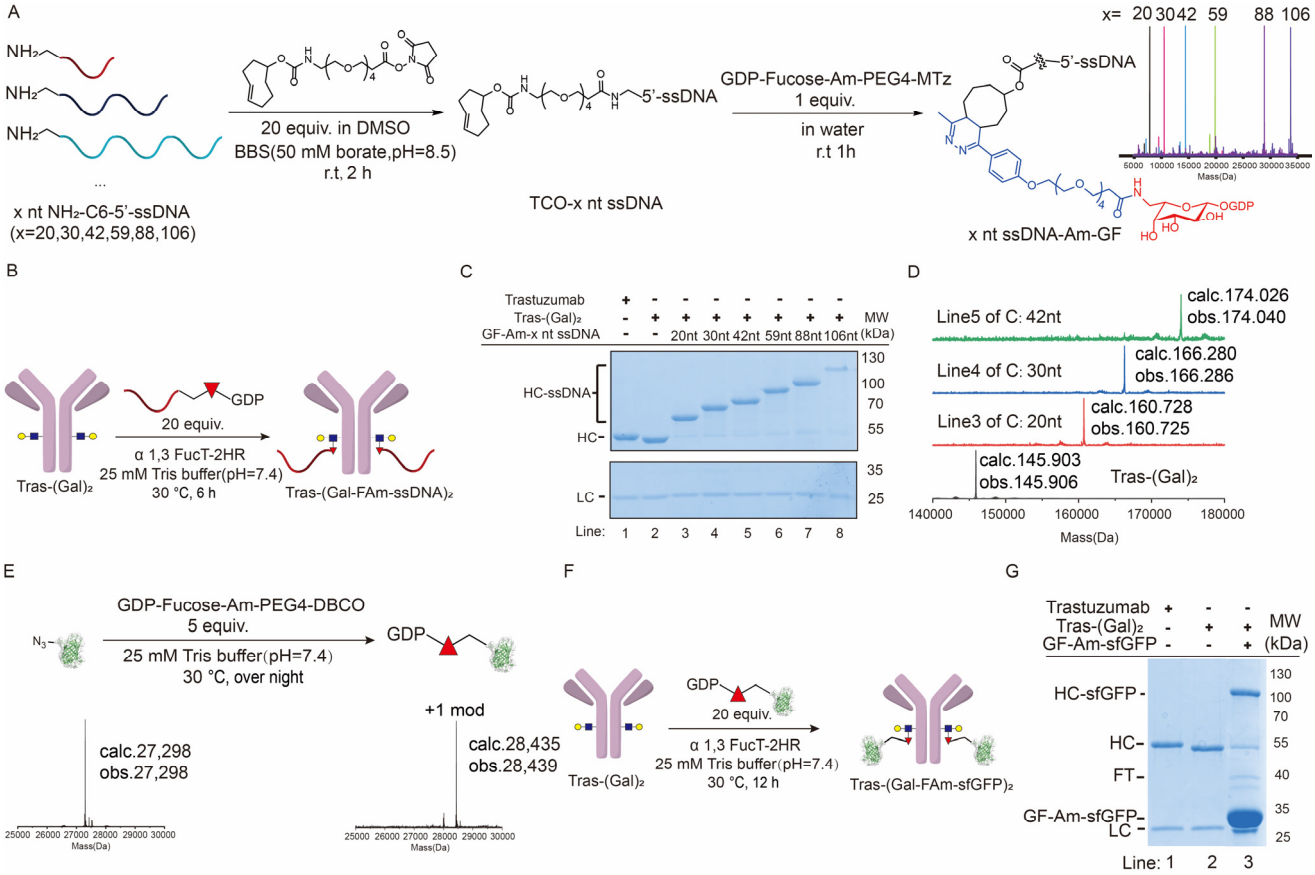


**Figure 5. Testing the payload capacity of LacNAc-Conju platform using different lengths of GDP-Fuc-ssDNA and GDP-Fucose-Am-sfGFP.** (A) Synthesis and ESI-MS characterization of GDP-Fucose-Am-x nt ssDNA (x=20, 30, 42, 59, 88, 106). (B) Schematic representation of the synthesis of Tras-(Gal-FAm-x nt ssDNA)$_2$ using Tras-A-LacNAc antibody as the model. (C) Evaluation of the conjugation efficacy by SDS-PAGE. Lane 1: reduced Trastuzumab (2 μg). Lane 2: reduced Tras-(Gal)$_2$ (2 μg). Lane 3-8: reduced crude conjugation products of Tras-(Gal-FAm-x nt ssDNA)$_2$ (2 μg) (x=20, 30, 42, 59, 88, 106). HC: heavy chain, LC: light chain. (D) ESI-MS analysis (after deconvolution) of the intact purified product of Tras-(Gal-FAm-x nt ssDNA)$_2$ made from Tras-(Gal)$_2$ in one-step (x=20, 30, 42). (E) Synthesis and ESI-MS characterization of GDP-Fucose-Am-sfGFP. (F) Schematic representation of the synthesis of Tras-(Gal-FAm-sfGFP)$_2$ using Tras-A-LacNAc antibody as the model. (G) Evaluation of the conjugation efficacy by SDS-PAGE. Lane 1: reduced Trastuzumab (2 μg). Lane

2: reduced Tras-$(Gal)_2$ (2 μg). Lane 3: reduced crude conjugation products of Tras-$(Gal\text{-}FAm\text{-}sfGFP)_2$ (2 μg). HC: heavy chain, LC: light chain. (obs: Observed; calc: Calculated)

In addition to the unexpected high efficiency of LacNAc-conju platform for modifying antibodies with small molecules, we explored the donor substrate tolerance of 1,3-FT-2TR to test the payload capacity of this platform. By increasing the molecular size of single-stranded DNA (ssDNA), we created a library of "molecular rules" ranging from 8,000 Da to 35,000 Da, which contain a 5' amine group for further modification (**Figure 5A**). After that, GDP-Fuc was introduced to these ssDNA probes (20 nt, 30 nt, 42 nt, 59 nt, 85 nt and 106 nt) via the combination of amine coupling and inverse-electron-demand Diels-Alder (iEDDA) reaction[30] and confirmed by LC-MS analysis (**Figure 5A** and **Figure S10**). Then we synthesized AOCs with these oligos using Tras-A-LacNAc antibody as the model, and tried to explore the maximal length of ssDNA that could be transferred by LacNAc-conju (**Figure 5B**). As revealed by SDS-PAGE gel analysis, nearly all the GDP-Fuc-ssDNA (134 μM) were completed converted with Tras-A-LacNAc (**Figure 5C and Figure S11A-B**). The specificity of Fc modification and the OAR was confirmed by the gel analysis and LC-MS analysis, suggesting only the heavy chains of antibodies were modified with one ssDNA probe specifically on the A-LacNAc (**Figure 5C-D and Figure S11C-F**). It is noteworthy that AOCs with long ssDNA (>50 nt) could not be characterized by LC-MS due to neutralized charges of antibody by the highly negatively charged oligos (**Figure S11G-J**). Aside from nucleic acids, GFP as the protein model was also introduced to GDP-Fuc to generate GDP-Fucose-Am-sfGFP (~27 kDa) (**Figure 5E and Figure S12A**), which was further transferred to Tras-A-LacNAc antibody by LacNAc-conju (**Figure 5F**). As expected, the result of SDS-PAGE confirmed that GFP was specifically modified on the A-LacNAc of the heavy chains of antibodies (**Figure 5G and Figure S12B**). Overall, we have demonstrated the excellent payload capacity of LacNAc-conju by increasing the size of payloads step by step, offering a general and versatile platform for one-step enzymatic transfer of biomacromolecules to Fc glycan homogeneously, which has been rarely reported.

**Construction and characterization of bispecific antibodies synthesized via LacNAc-conju**

After demonstrating that the LacNAc-conju platform allowed one-step transfer of biomacromolecules by FT to Fc in a site-specific and homogeneous manner, we applied it to construct

bispecific antibodies. Bispecific T cell engager, BiTE, is a type of bispecific antibody that has been leveraged to recruit cytolytic T cells for tumor killing. Specifically, T cells were activated by bispecific antibody-induced crosslinking of CD3 clustering on T cells as well as the target antigen on tumor cells[23]. As revealed by recent work, the molecular structure of bispecific or trispecific antibody is one the determinant of drug efficacy, especially for T cell engagers[31]. Chemical synthesizing multispecific antibody provides an alternative approach to design novel molecular structure for better cancer killing activity. Herein, we constructed bispecific antibodies targeting antigens of CD3 and HER2 via the LacNAc-conju platform. First, we expressed an anti-CD3 nanobody with a LPETGG tag at the C-terminus and engineered this nanobody with DBCO via the sortase A mediated ligation. After that, GDP-Fuc-AM-Azide (**6**) was allowed to react with DBCO-anti-CD3 nanobody, which generated anti-CD3 antibody-GDP-Fuc conjugates (GF-anti-CD3). The synthesized GF-anti-CD3 was confirmed by ESI-MS (**Figure 6A**). Subsequently, the bispecific antibody was constructed via the LacNAc-conju reaction between GF-anti-CD3 and Tras-A-LacNAc (Tras*anti-CD3) (**Figure 6B**). Results of SDS-PAGE and LC-MS characterization elaborated that the reaction attained high yield (>90%) (**Figure 6C-D**), indicating that we could realize highly efficient one-step transfer of proteins (~15 kDa) to antibody using LacNAc-conju, and provided a powerful tool for chemical construction of bispecific antibodies.

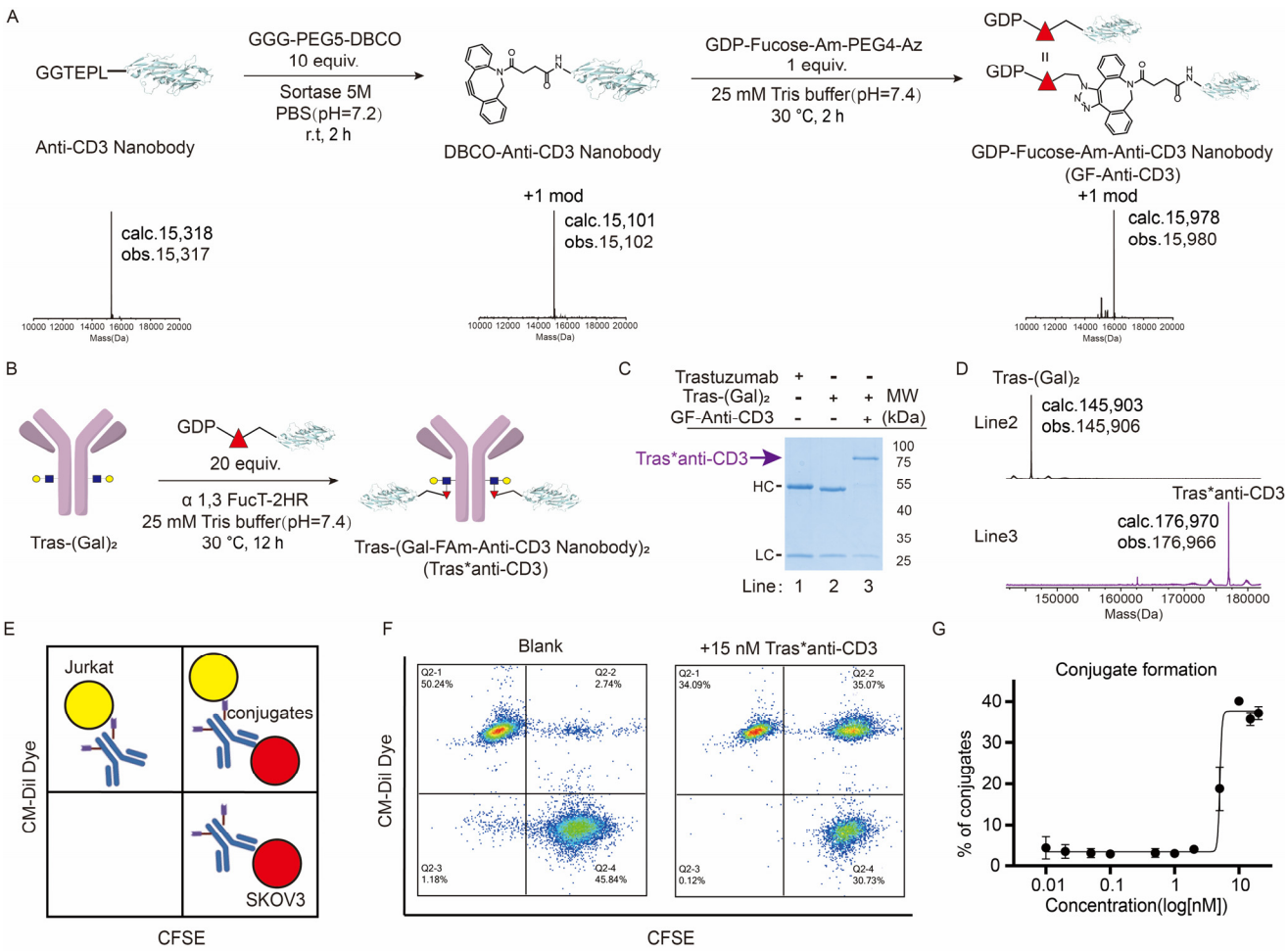


**Figure 6. Construction and characterization of HER2/CD3 bispecific antibodies by LacNAc-conju.** (A) Synthesis and ESI-MS characterization of GDP-Fuc-Am-antiCD3 nanobody. (B) Scheme of the synthesis of site-specific HER2/CD3 bispecific antibody, Tras-(Gal-FAm-AntiCD3 Nanobody)$_2$ (Tras*Anti-CD3), via LacNAc-conju. (C) SDS-PAGE analysis of purified Tras*Anti-CD3. Lane 1: reduced Trastuzumab (2 μg). Lane 2: reduced Tras-(Gal)$_2$ (2 μg). Lane 3: reduced purified Tras-AntiCD3 (2 μg). HC: heavy chain, LC: light chain. (D) ESI-MS analysis of the intact purified Tras*Anti-CD3 based on Tras-(Gal)$_2$. (E) Schematic of Tras*Anti-CD3-induced formation of conjugates. (F-G) Flow cytometric analysis of Tras*Anti-CD3-induced formation of conjugates. Unconjugated cells (upper left and lower right quadrants) display mono-positive fluorescence whereas conjugated cells (upper right quadrant) display dual-positive fluorescence. The conjugation formation frequency (right) was measured as the fraction of cells in the upper right region. Each point represents the average frequency with two technical replicates. Data are shown as means ± SD. (obs: Observed; calc: Calculated)

The functionality of Tras*anti-CD3 bispecific antibody was further characterized. First, the antigen-binding capability towards HER2 and CD3 was testified by flow cytometry analysis using SKOV3 cell lines (expressing human HER2 antigen) and Jurkat cell lines (expressing CD3 antigen), respectively (**Figure S13A-B**). The bispecific antibody showed comparable binding ability with unmodified trastuzumab, indicating that the constructed bispecific antibody maintained the inherent binding affinity of antibodies (**Figure S13A**). As for CD3, we found the enhanced binding ability of Tras*anti-CD3 in comparison with a single anti-CD3 nanobody, which could be attributed to the multivalency of two CD3 binding sites with structural stability on Tras*anti-CD3 (**Figure S13B**). Furthermore, we characterized the ability of bispecific antibody-mediated recruitment of T cells to cancer cells (**Figure 6E**). Jurkat cells (T cells) expressing CD3 antigen as well as SKOV3 cells (cancer cells) expressing human HER2 antigen were labelled with different fluorescent cell trackers, and then 15 nM Tras*anti-CD3 was added to induce the engagement. As expected, the ratio of cell conjugates was 16.9% without bispecific antibodies while up to 29.1% cell conjugates were formed by the addition of Tras*anti-CD3 (**Figure 6F**). Moreover, the frequency of cell conjugates increased with the increasing concentration of Tras*anti-CD3, indicating that the formation of bispecific antibody-mediated cell-cell conjugates was dose dependent (**Figure 6G**).

**Tras*anti-CD3 bispecific antibody induce selective killing of HER2 expressing cancer cells**

To testify the capability of bispecific antibodies to selective killing of cancer cells, we first chose human peripheral blood mononuclear cells (PBMCs) as the source of T cells to characterize the HER2 expressing cancer cells dependent activation of T cells under the treatment of Tras*anti-CD3 (**Figure 7A**). As expected, when PBMCs were co-cultured with SKOV3 cells (HER2+) in vitro, the expression levels of T cell activation marker CD69 and CD25 along with the amounts of cytotoxic cytokines (IFN-γ and TNF-α) were upregulated for both of CD4+ and CD8+ T cells in the presence of bispecific antibodies (**Figure 7B-C and Figure S13C-D**). Conversely, weak activation was observed for T cells alone after the incubation with Tras*anti-CD3, which was consistent with the previous report[23], indicating that the bispecific antibody-mediated T cell activation was antigen-dependent.

Afterwards, we tested the *in vitro* cytotoxicity of bispecific antibodies towards HER2+ SKOV3 cells. The cell growth curves of SKOV3 cells under different treatments were monitored. Interestingly,

cancer cells incubated with Tras*anti-CD3 and PBMCs were significantly killed, and the simple mixture of trastuzumab with anti-CD3 nanobody or trastuzumab alone also induced significant but slighter inhibition on the growth of SKOV3 cells, while the other groups were hardly influenced (**Figure 7D**). Different from Tras*anti-CD3, trastuzumab induced cell killing mainly via ADCC. The results suggest that the successful engagement between cancer cells and T cells are quite important for the potent killing. For comparison, we also monitored the viability of MDA-MB-468 cell lines without HER2 expression under same treatments. As a result, the growth of MDA-MB-468 cells were almost unaffected under all of the treatments, confirming that the bispecific antibody-mediated T cell cytotoxicity was antigen-dependent (****$P<0.0001$) (**Figure 7E**).

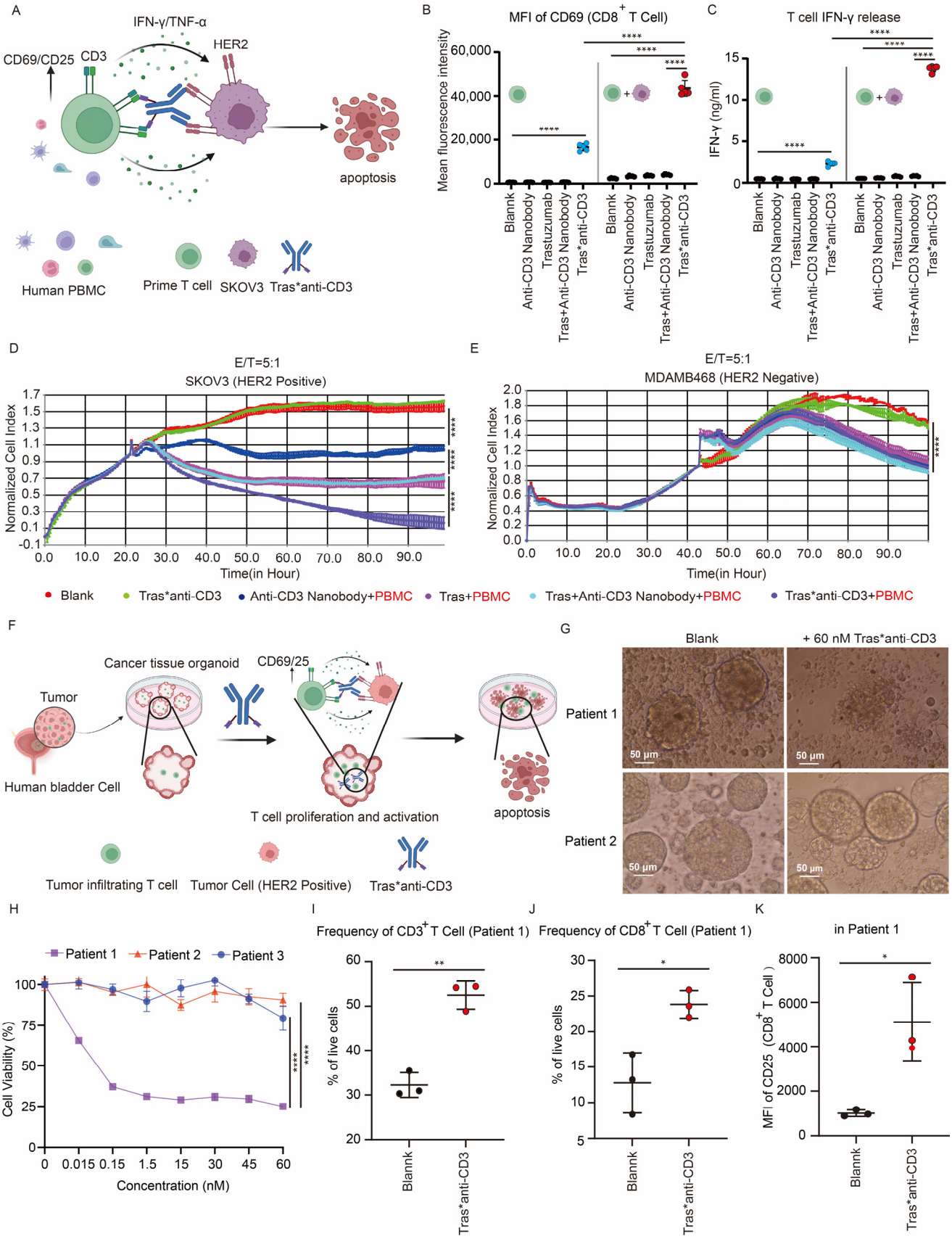


**Figure 7. Specific immune activation and cancer killing mediated by Tras*anti-CD3 as a T cell engager.** (A) Schematic representation for Tras*anti-CD3 mediated cytolytic T cells and cancer cell

engagement. (B-C) Flow cytometric analysis of CD69 expression levels of $CD8^+$ T cells and (C) the IFN-γ cytokine secretion measured by ELISA (right) after 48 hours of coculture of PBMC and SKOV3 cells under the treatment (Student's *t* test, ****P<0.0001, n=5). (D-E) Real-time monitoring of the viability of target cells (SKOV3 and MDAMB-468) by X-CELLigence RTCA DP technology (2-way ANOVA, ****P<0.0001, n=3). SKOV3 cells (left) and MDAMB-468 cells (right) were independently plated in 16-well E-plates at 10,000 cells/well and 20,000 cells/well, respectively. PBMCs (effector cells/T cells (E/T) =5) were added after target cells were incubated for 24 h (SKOV3) or 42 h (MDAMB-468) at 37°C and the impedance was measured at intervals of 15 min. (F) Schematic representation of the efficacy of Tras*anti-CD3 on human tumor organoids for tumor killing. (G) Bright field images of Tras*anti-CD3 induced cancer cell killing towards the organoids from different patients. Scale bar: 50 μm. (H) Cell viability of the organoids from different patients (2-way ANOVA, ****P<0.0001, n=3). HER2+ cells with T cells, HER2+ cells without T cells and HER2- cells without T cells were collected from patients 1-3, respectively. Data are shown as means ± SD. (I-J) The proportion of CD3+ T cells (I) and CD8+ T cells (J) of patient 1 after the induction of Tras*anti-CD3 (Student's *t* test, *P<0.05, **P<0.01, n=3). (K) CD25 expression levels of $CD8^+$ T cells of patient 1 after the induction of Tras*anti-CD3 (Student's *t* test, *P<0.05, n=3).

Finally, we evaluated the efficacy of Tras*anti-CD3 on patient-derived HER2+ cancer organoids of bladder cancer to test its tissue penetration ability (**Figure 7F**). Noteworthily, we used an optimized Matrigel-free system to maintain the organoid and the tumor infiltrating T cells could be preserved for several days inside organoid. Organoids from three patients (patient 1-3: HER2+ cells with T cells, HER2+ cells without T cells, HER2- cells without T cells) (**Figure S13A-C**) were constructed and treated with Tras*anti-CD3. As expected, bright-field images and cell viability analysis demonstrated that 60 nM Tras*anti-CD3 induced significantly tumor killing towards the tumor cells of patient 1 with both HER2+ cells and T cells, whereas it hardly influenced the tumor cells of other patients (****P<0.0001) (**Figure 7G-H and Figure S13D**), which coincided with the result of cell lines and demonstrated that the engagement between cancer cells and T cells were crucial for tumor killing. Moreover, after the induction of Tras*anti-CD3, the frequency of CD3+ T cells increased significantly (**P<0.01) (**Figure 7I and Figure S13E**), indicating that Tras*anti-CD3 induced T cell proliferation

for tumor killing. Likewise, the significant rise of CD8+ T cells indicated that cytotoxic T cells dominated the tumor killing (*P<0.05) (**Figure 7J and Figure S13F**). Furthermore, the expression level of CD25 was significantly upregulated on CD8+ T cells (*P<0.05), suggesting that Tras*anti-CD3 had the potential ability to recruitment of cytolytic T cells for tumor killing in deep tissue (**Figure 7K**).

**Discussions and outlook.**

Site-specific modification of native IgG molecules is more and more customized in modern bio-technologies in attempt to meet the rapidly evolving applications. Thus, chemical tools for rapid engineering of native antibodies are still in demand for both of fundamental and translational research. Glycoengineering is the one of the most convenient methods for the site-specific modification of native or commercial IgG antibodies into homogeneous conjugates. However, most of current enzymatic glycoengineering take hours to days to complete the full conversion. Conventional explanations for the slow reaction rate of enzymatic Fc glycoengineering are attributed to the unfavorable structure of donor substrate derivatives. Thus, engineering of glycosyltransferases (GTs) and optimization of donor substrate's chemical structure are the main directions to increase the reaction rate.

In this work, we demonstrated that, despite being valuable, optimization of GT and donor substrate only improve the unnatural fucosylation at a certain level. By contrast, reducing the complexity of Fc glycan, as the remodeling of acceptor substrates, could boost the reaction dramatically. More broadly, the monoantennary LacNAc structure could be introduced onto proteins beyond antibody, such as at the C terminal of anti-PD-L1 nanobody, and then it could be recognized as a glycan tag by FT enzyme. We demonstrated the single LacNAc unit introduced onto anti-PDL1 nanobody could be further modified by GDP-Fuc-AM-biotin with the conversion efficiency of 95% within 1 min **(Figure S14)**, suggesting LacNAc might be a glycan tag for enzymatic "click reaction".

Another advantage of LacNAc-conju platform is the broad payload capacity. The great donor substrate tolerance of 1,3FT-2TR as well as the simple acceptor substrate of A-LacNAc make the unexpected direct enzymatic transfer of biomacromolecules. Meanwhile, it is not just a saturated labeling, but a full conversion to provide homogeneous AOC or bispecific antibody. It is anticipated that LacNAc-conju platform can be applied for making novel conjugates for imaging, nanofabrication,

biosensing as well as therapeutics. The direct enzymatic transfer of biomacromolecules to antibody via LacNAc-conju uses LacNAc and GDP-Fuc as reaction handles, both of which are much more hydrophilic than common bioorthogonal handles. This unique property might help to accelerate the conjugation with very hydrophobic, e.g., toxin, and/or large size moieties, e.g., cytokines, because of the increasement of payload solubility or the easily exposed reaction handles are in aqueous buffer.

Finally, we have applied the developed LacNAc-conju platform for constructing ADC and bispecific antibody, and demonstrated their excellent pharmaceutical property and efficacy in mice model or patient derived organoid. The novel molecular structure of antibody conjugates from LacNAc-conju platform provide great opportunities for AXC drug development. Ongoing efforts for further clinical translation of this technique focus on developing appropriate processing, such as enzyme fusions and immobilization.

## Competing financial interests

Several patent applications were filed by Glyco-therapy Biotechnology Co., Ltd. and/or Nanjing University.

## Additional information

Correspondence and requests for materials should be addressed to J.P.L or Y.Y.

## References


1. Beck, A., Goetsch, L., Dumontet, C. & Corvaia, N. Strategies and challenges for the next generation of antibody-drug conjugates. *Nat Rev Drug Discov* **16**, 315-337 (2017).
2. Modi, S. *et al.* Trastuzumab Deruxtecan in Previously Treated HER2-Low Advanced Breast Cancer. *N Engl J Med* **387**, 9-20 (2022).
3. Mullard, A. Antibody-oligonucleotide conjugates enter the clinic. *Nat Rev Drug Discov* **21**, 6-8 (2022).
4. Pan, L., Cao, C., Run, C., Zhou, L. & Chou, J.J. DNA-Mediated Assembly of Multispecific Antibodies for T Cell Engaging and Tumor Killing. *Adv Sci (Weinh)* **7**, 1900973 (2020).
5. Stoeckius, M. *et al.* Simultaneous epitope and transcriptome measurement in single cells. *Nat Methods* **14**, 865-868 (2017).
6. Robinson, P.V., Tsai, C.T., de Groot, A.E., McKechnie, J.L. & Bertozzi, C.R. Glyco-seek: Ultrasensitive Detection of Protein-Specific Glycosylation by Proximity Ligation Polymerase Chain Reaction. *J Am Chem Soc* **138**, 10722-10725 (2016).

7. Wang, B. *et al.* Potent and Prolonged Innate Immune Activation by Enzyme-Responsive Imidazoquinoline TLR7/8 Agonist Prodrug Vesicles. *J Am Chem Soc* **142**, 12133-12139 (2020).
8. Carter, P.J. & Lazar, G.A. Next generation antibody drugs: pursuit of the 'high-hanging fruit'. *Nat Rev Drug Discov* **17**, 197-223 (2018).
9. Agarwal, P. & Bertozzi, C.R. Site-specific antibody-drug conjugates: the nexus of bioorthogonal chemistry, protein engineering, and drug development. *Bioconjug Chem* **26**, 176-192 (2015).
10. Dickgiesser, S. *et al.* Site-Specific Conjugation of Native Antibodies Using Engineered Microbial Transglutaminases. *Bioconjugate Chem* **31**, 1070-1076 (2020).
11. Wacker, C., Berger, C.N., Girard, P. & Meier, R. Glycosylation profiles of therapeutic antibody pharmaceuticals. *Eur J Pharm Biopharm* **79**, 503-507 (2011).
12. van Geel, R. *et al.* Chemoenzymatic Conjugation of Toxic Payloads to the Globally Conserved N-Glycan of Native mAbs Provides Homogeneous and Highly Efficacious Antibody-Drug Conjugates. *Bioconjug Chem* **26**, 2233-2242 (2015).
13. Zeglis, B.M. *et al.* Enzyme-mediated methodology for the site-specific radiolabeling of antibodies based on catalyst-free click chemistry. *Bioconjug Chem* **24**, 1057-1067 (2013).
14. Li, X., Fang, T. & Boons, G.J. Preparation of well-defined antibody-drug conjugates through glycan remodeling and strain-promoted azide-alkyne cycloadditions. *Angew Chem Int Ed Engl* **53**, 7179-7182 (2014).
15. Huang, W., Giddens, J., Fan, S.Q., Toonstra, C. & Wang, L.X. Chemoenzymatic glycoengineering of intact IgG antibodies for gain of functions. *J Am Chem Soc* **134**, 12308-12318 (2012).
16. Tang, F. *et al.* One-pot N-glycosylation remodeling of IgG with non-natural sialylglycopeptides enables glycosite-specific and dual-payload antibody-drug conjugates. *Org Biomol Chem* **14**, 9501-9518 (2016).
17. Parsons, T.B. *et al.* Optimal Synthetic Glycosylation of a Therapeutic Antibody. *Angew Chem Int Ed Engl* **55**, 2361-2367 (2016).
18. Li, C. *et al.* Site-Selective Chemoenzymatic Modification on the Core Fucose of an Antibody Enhances Its Fcgamma Receptor Affinity and ADCC Activity. *J Am Chem Soc* **143**, 7828-7838 (2021).
19. Shi, W. *et al.* One-step synthesis of site-specific antibody-drug conjugates by reprograming IgG glycoengineering with LacNAc-based substrates. *Acta Pharm Sin B* **12**, 2417-2428 (2022).
20. Zhang, X. *et al.* Site-Specific Chemoenzymatic Conjugation of High-Affinity M6P Glycan Ligands to Antibodies for Targeted Protein Degradation. *Acs Chemical Biology* (2022), DOI: https://doi.org/10.1021/acschembio.1c00751.
21. Zhang, X. *et al.* General and Robust Chemoenzymatic Method for Glycan-Mediated Site-Specific Labeling and Conjugation of Antibodies: Facile Synthesis of Homogeneous Antibody-Drug Conjugates. *ACS Chem Biol* **16**, 2502-2514 (2021).
22. Li, J. *et al.* A Single-Step Chemoenzymatic Reaction for the Construction of Antibody-Cell Conjugates. *ACS Cent Sci* **4**, 1633-1641 (2018).
23. Brinkmann, U. & Kontermann, R.E. Bispecific antibodies. *Science* **372**, 916-917 (2021).
24. Yin, S.Y. *et al.* Patient-derived tumor-like cell clusters for drug testing in cancer therapy. *Science Translational Medicine* **12**, eaaz1723 (2020).

25. Sun, H.Y. *et al.* Structure and mechanism of Helicobacter pylori fucosyltransferase. A basis for lipopolysaccharide variation and inhibitor design. *J Biol Chem* **282**, 9973-9982 (2007).
26. Lin, Y.-N. *et al.* Chemoenzymatic Synthesis of GDP-L-Fucose Derivatives as Potent and Selective α-1,3-Fucosyltransferase Inhibitors. *Advanced Synthesis & Catalysis* **354**, 1750-1758 (2012).
27. Cobb, B.A. The history of IgG glycosylation and where we are now. *Glycobiology* **30**, 202-213 (2020).
28. Agard, N.J., Prescher, J.A. & Bertozzi, C.R. A strain-promoted [3+2] azide-alkyne cycloaddition for covalent modification of biomolecules in living systems (vol 126, pg 15046, 2004). *Journal of the American Chemical Society* **127**, 11196-11196 (2005).
29. Kolodych, S. *et al.* Development and evaluation of beta-galactosidase-sensitive antibody-drug conjugates. *Eur J Med Chem* **142**, 376-382 (2017).
30. Blackman, M.L., Royzen, M. & Fox, J.M. Tetrazine ligation: fast bioconjugation based on inverse-electron-demand Diels-Alder reactivity. *J Am Chem Soc* **130**, 13518-13519 (2008).
31. Santich, B.H. *et al.* Interdomain spacing and spatial configuration drive the potency of IgG-[L]-scFv T cell bispecific antibodies. *Science Translational Medicine* **12**, eaax1315 (2020).